Sensors & Transducers

Intelligent Sensing in Inverter-fed Induction Motors: Wavelet-based Symbolic Dynamic Analysis

[1]Rohan SAMSI, [2]Asok RAY

[1]Primarion Inc. 2780 Skypark Drive, Suite 100 Torrance, CA 90505
[2]The Pennsylvania State University, 329 Reber Building, University Park, PA 16802
E-mail: rohan.samsi@primarion.com, axr2@psu.edu

Abstract: Wavelet transform allows adaptive usage of windows to extract pertinent information from sensor signals, and symbolic dynamic analysis provides coarse graining of the underlying information for enhanced computational speed and robustness of sensor-data-driven decision-making. These two concepts are synergistically combined for real-time intelligent sensing of faults whose signatures are small compared to coefficients of dominant frequencies in the signal. Feasibility of the proposed intelligent sensing method is demonstrated on an experimental apparatus for early detection of rotor bar breakage in an inverter-fed induction motor. *Copyright © 2008 IFSA.*

1. Introduction

Wavelet transform is a powerful tool for multi-scale representation of non-stationary signals. Wavelet analysis allows adaptive usage of long windows for retrieving low frequency information and short windows for high frequency information [1]. This property is particularly critical for detection of faults that manifest at multiple frequencies. The ability to perform flexible localized analysis is one of the striking features of the wavelet transform. Hence, they have been extensively used for fault detection [2]. A symbolic dynamic approach to fault detection was first introduced in [3] and later has been experimentally validated in different applications [4-6]. An important practical advantage of working with symbols is that the efficiency of numerical computations is significantly enhanced over what it would be for the original data; this is critical for real-time monitoring and control applications. Another advantage is that analysis of symbolic data is often less sensitive to measurement noise. Therefore, applications of symbolic methods are favored in circumstances where robustness to noise, speed, and/or cost is of paramount importance [7].

This paper presents an application that combines the merits of wavelet transform and symbolic dynamic analysis for intelligent sensing of both gradually evolving and abrupt faults. In this context, the problem of detecting broken rotor bars in three-phase squirrel-cage induction motors is investigated. The analysis of broken rotor bars, in line-fed motors, has been well studied [8]. In the experimental apparatus, reported in this paper, an induction motor is operated as part of an open loop V/Hz drive system; these drive systems are used in various applications such as locomotives and cranes. Detection of rotor bar faults becomes difficult due to the inverter harmonics that tend to mask the fault signatures [9]. This information needs to be identified, extracted and represented properly in order to provide an appropriate assessment of the motor's health status.

The paper is organized into six sections including the present section. Section II presents the basic principles of wavelet transform analysis as needed for analysis in subsequent sections. The concept of symbolic dynamic analysis that is recently reported in literature [3] is briefly described in Section 3. Section 4 analyzes the effects of induction motor currents with broken rotor bars that generate additional harmonics in the line frequency. Section 5 describes the experimental apparatus and discusses the results on detection of broken rotor bars. Section 6 summarizes and concludes the paper with recommendations for future research.

2. Wavelet Transform Analysis

Preprocessing of time series data is often necessary for extraction of pertinent information. Although Fourier analysis is adequate if the signal to be analyzed is stationary and if the time period is accurately known. Therefore, Fourier analysis may not be appropriate for non stationary signals (e.g., signals subjected to drifts, abrupt asynchronous changes and frequency trends). Wavelet analysis alleviates these difficulties via adaptive usage of long windows for retrieving low frequency information and short windows for high frequency information [1]. The ability to perform flexible localized analysis is one of the striking features of wavelet transform.

In multi-resolution analysis (MRA) of wavelet transform [10], a continuous signal $f \in \mathbb{H}$, where $\mathbb{H}$ is a Hilbert space, is decomposed as a linear combination of time translations of scaled versions of a suitably chosen scaling function $\phi(t)$ and the derived wavelet function $\psi(t)$. Let the sequence $\{\phi_{j,k}\}$ belong to another Hilbert space $\mathbb{M}$ with a countable measure, where the scale $s = 2^j$ and time translation $\tau = 2^{-j}k$. If the sequence $\{\phi_{j,k}\}$ is a frame for the Hilbert space $\mathbb{H}$ with a frame representation operator $\mathbb{L}$, then there are positive real scalars A and B such that:

$$A||f||_{\mathbb{H}}^2 \leq ||\mathbb{L}f||_{\mathbb{M}}^2 \leq B||f||_{\mathbb{H}}^2 \quad \forall f \in \mathbb{H}, \tag{1}$$

where $\mathbb{L}f = \{< f, \phi_{j,k} >\}$ and $||\mathbb{L}f||_{\mathbb{M}}$ is an appropriate norm, e.g., $||\mathbb{L}f||_{\mathbb{M}} = \sqrt{\sum_j \sum_k |< f, \phi_{j,k} >|^2}$ is a candidate norm; and $< x, y >$ is the inner product of x and y, both belonging to $\mathbb{H}$.

The above relationship is a norm equivalence and represents the degree of coherence of the signal f with respect to the frame set of scaling functions; it may be interpreted as enforcing an approximate energy transfer between the domains $\mathbb{H}$ and $\mathbb{L}(\mathbb{H})$. In other words, for all signals $f \in \mathbb{H}$, a scaled amount of energy is distributed in the coefficient domain where the scale factor lies between A and B[1]. However, the energy distribution is dependent on the signal's degree of coherence with the underlying frame $\{\phi_{j,k}\}$. For a signal f, which is coherent with respect to the frame $\{\phi_{j,k}\}$, norm equivalence in the frame representation necessarily implies that a few coefficients contain most of the signal energy and hence have relatively large magnitudes. Similarly, pure noise signal w being incoherent with respect to the set $\{\phi_{j,k}\}$, must have a frame representation in which the noise energy is

spread out over a large number of coefficients. Consequently, these coefficients have a relatively small magnitude. The orthogonal wavelets, utilized for analysis, form a tight frame with $A = B = 1$ [10].

Let $\tilde{f}$ be a noise-corrupted version of the original signal f expressed as:

$$\tilde{f} = f + \sigma \, w, \tag{2}$$

where w is additive white Gaussian noise with zero mean and unit variance and σ is the noise level. Then, the inner product of $\tilde{f}$ and $\phi_{j,k}$ is obtained as:

$$< \tilde{f}, \phi_{j,k} > = \underbrace{< f, \phi_{j,k} >}_{signal\ part} + \sigma \underbrace{< w, \phi_{j,k} >}_{noise\ part}. \tag{3}$$

The noise part in Eq. (3) may further be reduced if the basis and the scales over which coefficients are obtained are properly chosen.

2.1. Selection of the Wavelet Basis

Several properties of a wavelet determine its suitability as a basis. Much depends on the characteristics of the signal like frequency trends and discontinuities. The properties that are relevant to the problem of detecting broken rotor bars are discussed below.

- *Time-Frequency Localization*: Localization in time facilitates identification of abrupt changes in the temporal behavior. In contrast, localization in frequency is essential for identification of faults in narrow frequency bands. For example, the 'db1' or 'Haar' wavelet basis is well localized in time, whereas the 'sinc' wavelet is well localized in frequency [1]. In general, Wavelets with compact support yield good time localization.

- *Vanishing moments*: Vanishing moments of the wavelet are related to its ability to suppress oscillations. For example, if the wavelet basis has $p + 1$ vanishing moments, it will suppress all polynomials of degree p. Therefore, a wavelet basis with large number of vanishing moments tends to capture the change in the "higher-order" of power-series decomposition. Since faults are usually associated with higher order terms; this property will ensure that even small faults will not go undetected.

- *Regularity*: Regularity defines smoothness of the wavelet basis and is useful for separating the frequency components in the fault signals. This property is derived from vanishing moments.

- *Symmetry*: This property is useful for factoring out phase information that may lead to false alarms. Enforcing symmetry causes the wavelet basis to be a complex function. In fact, except the 'Haar' wavelet, there is no other compactly supported wavelet is symmetric [1].

Many wavelets may satisfy one or more of the above desirable properties. In such a case, it is advantageous to choose a wavelet basis that is coherent with the signal. A measure of coherence between the signal and wavelet could be obtained from their cross-correlation that is defined as:

$$\Gamma_{f,\psi_\alpha} = \frac{< f, \psi_\alpha >}{||f||_2 ||\psi_\alpha||_2}, \tag{4}$$

where f is the signal and ψ_α is the suitably scaled wavelet. $< f, \psi_\alpha >$ is the inner product between the

vectors f and ψ_α and $||f||_2$ is the Euclidean norm of f.

2.2. Selection of the Wavelet Scales

For every wavelet, there exists a certain frequency called the center frequency F_c that has the maximum modulus in the Fourier transform of the wavelet [11]. As an example, Fig. 1 depicts the center frequency associated with the Daubechies wavelet 'db4'.

For a given scale α and the sampling interval Δt, the pseudo-frequency f_p^α of the wavelet is defined as [11]:

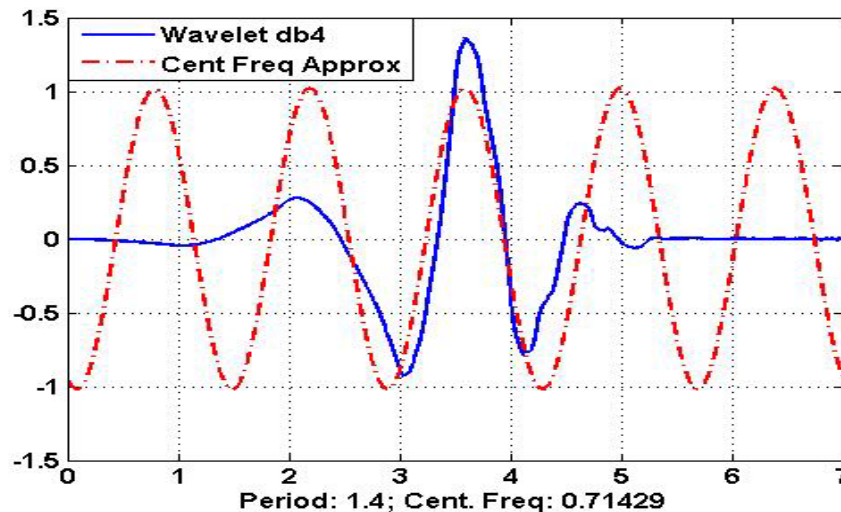$$f_p^\alpha = \frac{F_c}{\alpha \, \Delta t} \qquad (5)$$

Fig. 1. Center Frequency Approximation for Wavelet db4.

The wavelet coefficients of a signal have the maximum magnitude at the scale corresponding to the pseudo-frequency. Hence, it would be appropriate to choose scales such that the pseudo-frequency corresponds to the frequency of interest. Multiple scales can be chosen as per Eq. (5) if necessary.

2.3. Discrete Wavelet Transform

The Continuous Wavelet Transform (CWT) of a signal $f(t)$ is defined as:

$$CWT_{\alpha,\tau} = \alpha^{-1/2} \int_{-\infty}^{\infty} f(t)\psi\left(\frac{t-\tau}{\alpha}\right)dt , \qquad (6)$$

where $\psi(t)$ is the mother wavelet with $\alpha > 0$ being the scale and τ being the time shift. The *average* and *detail* coefficients of DWT are obtained as:

$$
\begin{aligned}
C(j,k) &= 2^{-j/2} \int_{-\infty}^{\infty} f(t)\psi(2^{-j}t - k)dt \\
D_j(t) &= \sum_{k\in\mathbb{Z}} C(j,k)\psi_{j,k}(t)
\end{aligned}
\tag{7}
$$

A combination of the above equation pair yields an expression for computation of the *detail* coefficients of DWT as:

$$
D_j(t) = \sum_{k\in\mathbb{Z}} 2^{-j/2} \int_{-\infty}^{\infty} f(t)\psi(2^{-j}t - k)dt\,\psi_{j,k}(t)
\tag{8}
$$

Computation of the DWT *detail* coefficients in Eq. (9) is computationally more efficient than that of the CWT coefficients in Eq.(9) because a filter-bank implementation is used for computing DWT [1]. Only orthogonal wavelets have been used in this paper as these wavelets have tight frames and hence reduce the computational load. Unless the signal to be analyzed exhibits fractal behavior, DWT at dyadic scales are adequate.

Enforcing the orthogonality conditions causes the wavelet transform to lose its shift-invariance [12]. Symbolic dynamics partially mitigate this limitation by extracting the statistical properties of the signal.

3. Symbolic Analysis of Wavelet Coefficients

Application of Symbolic Dynamic Filtering (SDF) to fault detection in complex dynamical systems has been introduced in [3], where the space of continuous wavelet coefficients is partitioned to generate symbols. Various aspects of symbol generation with wavelet coefficients, such as the selection of the alphabet size and the advantages of using wavelet coefficients with regard to noise mitigation and robustness are discussed in [13]. The Maximum Entropy (*ME*) scheme of partitioning introduced in [13] is presented briefly below.

Let N be the length of the data sequence and $|\Sigma|$ be the cardinality of the (finite) alphabet Σ. The data set is sorted in the ascending order. Starting from the first point in the sorted set, every consecutive segment of length $\left\lfloor \frac{N}{|\Sigma|} \right\rfloor$ forms a distinct element of the partition, where $\lfloor x \rfloor$ represents the greatest integer less than or equal to x. Each partition is then labeled with one symbol from the alphabet. If the data point lies in a particular region, it is coded with the symbol associated with that region. Thus, a sequence of symbols is created from a sequence of wavelet-transformed time series data, hereafter called *scale series* data.

With such a partition, a region with large information content is allocated more symbols and hence a finer partitioning is achieved in such a region. Similarly, a region with sparse information content is allocated fewer symbols and hence a coarser partitioning is achieved in such a region. Thus, even small changes in the system behavior will be reflected in the symbol sequence obtained under *ME* partitioning.

The discrete wavelet coefficients are obtained for various dyadic scales. The detail coefficients are stacked to obtained the scale series. The scale series data corresponding to normal condition is partitioned with maximum entropy scheme to generate the partitions. These partitions remain invariant for all conditions. The probability distribution of the symbols represents the status of the system at any given time. As the fault occurs, the characteristics of the signal change and this is reflected in the wavelet coefficients. The symbol sequence generated from the coefficients also changed and so do

their probabilities. In order to quantify change, a scalar measure is induced on the probability distributions, denoted as an anomaly measure M. One such measure of anomaly is $M_k = d(\mathbf{p}^k, \mathbf{p}^1)$ where $\mathbf{p}^1$ is the probability distribution corresponding to the reference test #1 and $\mathbf{p}^k$ is the current probability distribution for the test #k; and $d(\bullet, \bullet)$ is a scalar distance between two probability vectors of the same dimension. The relative entropy or the Kullback-Leibler distance [14] has been found suitable as the measure of anomaly in this paper. It is noted that there are other alternative choices of the distance function for the anomaly measure [3].

4. Fault Analysis in Induction Motors

Analysis of three-phase induction motor currents with broken rotor bars yields additional frequency components in the line frequency [8].

$$F = f \left[\frac{K}{P}(1 - s) \pm s \right], \tag{9}$$

where f, P and s are, respectively, the electrical supply frequency, number of pole pairs, and the per-unit slip; $K/P = 1, 3, 5, 7, 11, 13, \ldots$ due to the normal winding configuration. For $K/P = 1$, the additional components in the current spectrum are $(1 - 2s)f$, due to the broken rotor bar, and $(1 + 2s)f$, owing to the speed oscillations. In the case of line-fed machines, the frequency f is usually 60 Hz. Inverters introduce harmonics due to the switching action. The harmonics introduced have the following frequencies $(2m + 1)f$, where $m = 0, 1, 2 \ldots$. Since the motor under investigation is 3-phase, triple harmonics are eliminated. So the harmonics present in the stator current waveform are $f, 5f, 7f, 11f, 13f, \ldots$. The higher harmonics are weighted by $\frac{1}{m}$ where m is the harmonic number, so harmonics beyond 15 are ignored. In this way, several frequency bands are available for analysis of fault signatures.

The following transform is used to obtain the direct axis and quadrature axis currents.

$$i_d = \frac{\sqrt{2}}{\sqrt{3}} i_A - \frac{1}{\sqrt{6}} i_B - \frac{1}{\sqrt{6}} i_C$$

$$i_q = \frac{1}{\sqrt{2}} i_B - \frac{1}{\sqrt{2}} i_C$$

The Parks vector modulus $|i_d + ji_q|^2$ is then calculated. If there are broken rotor bars, the fault signatures can be seen at $2sf, 4sf, 10sf, 20sf \ldots$, where s is the per-unit slip. The fault signature for the fundamental component is expected to be at least 30 to 50 dB below the DC component. This number is larger for the higher harmonics and that is why rotor bar breakages are difficult to detect.

5. Experimental Apparatus and Test Results

This section describes the experimental apparatus for detection of broken rotor bar(s) in induction motors and discusses the associated test results.

5.1. Description of the Experimental Apparatus

The motors under test belong to the class of 3-phase, 2-HP Y-connected squirrel cage induction

machines, and are driven by a commercial-grade inverter in the open-loop V/Hz mode. The motors are loaded to a desired level by a hysteresis dynamometer (model HD-805 6N manufactured by Magtrol) through a flexible Lovejoy coupling.

The sensing board consists of both voltage and current sensors, followed by operational amplifiers. These amplifiers provide sufficient gain as needed for data acquisition on a dSPACE DS-1103 PPC card having sixteen 14-bit ADC units, four 12-bit ADC units, and eight 12-bit DAC outputs. The bandwidth of the sensors are intentionally kept wide so that both high-frequency and low-frequency harmonics could be measured and analyzed.

The rotors are made of solid aluminum construction and the rotor bars are embedded in the laminate. To break a rotor bar, a hole was milled deep and wide enough into the laminate such that it broke one rotor bar. This ensures the disruption of the current path in one of the bars. Experiments were conducted with tests on ten identical motors, of which five were healthy and the remaining five were made faulty with a single broken bar to emulate the faulty condition. The load on the motor was set to 3Nm and the slip was observed to be $\frac{1}{60}$ for all ten test cases. The currents were sampled at a frequency of $10\ kHz$ and the test data were acquired for 45 seconds. Out of a total of $450,000$ data points for each test, only 25 seconds of data between the 10th and 35th second was selected for fault analysis to assure statistical stationarity.

5.2. Test Results and Discussion

The Daubechies family of wavelets satisfies many of the requirements mentioned in Section 2 and their salient features are:
- Orthogonality and compact support;
- Existence of several vanishing moments; and
- Time-frequency localization.

In this paper, standard Daubechies wavelets, 'db3', 'db4', 'db5', 'db6', 'db7', 'db8' and 'db10', have been considered as possible candidates for the wavelet basis. Table 1 lists the values of correlation Γ between the wavelets and the measured signal.

Table 1. Cross Correlation Values.

Wavelet	Correlation Γ
$db3$	0.3353
$db4$	0.3414
$db5$	0.3108
$db6$	0.2355
$db7$	0.2145
$db8$	0.2065
$db10$	0.2551

Since the wavelet 'db4' has the largest value of the correlation Γ among all the wavelets under consideration, it was chosen as the basis in the analysis. The rotor bar breakage faults manifest at frequencies mentioned in Section 4. The wavelet scales are calculated by substituting these frequencies in place of the pseudo-frequency f_p in Eq. (5). In DWT, these scales correspond to decomposition levels 11 and 12.

Wavelet decomposition has been performed on the acquired data and *detail* coefficients corresponding to levels 11 and 12 are considered for symbolic analysis. As typical examples, the *detail* coefficients [1] are shown in Fig. 2, where the top and bottom plates correspond to profiles of wavelet coefficients for test #1 (healthy motor) and test #6 (faulty motor), respectively. The wavelet coefficients are significantly different from each other and hence the choice of 'db4' is appropriate as it is capable of distinguishing between healthy and faulty motors.
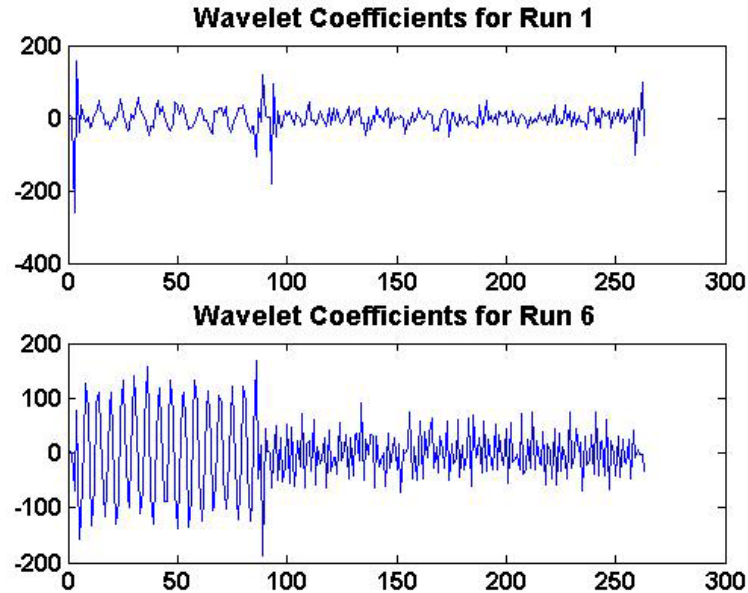
Fig. 2. Plot of Discrete Wavelet Coefficients.

The alphabet size $|\Sigma|$ was chosen to be eight. The *detail* coefficients for test #1 (healthy motor) are stacked to form a set of scale series data that is partitioned under the maximum entropy (*ME*) criterion [13] as shown in Fig. 3. This partition remains invariant in the further analysis for faulty conditions. With the *ME* partition generated above, symbol sequences are generated from wavelet coefficients for all remaining runs, i.e., test #2 to test #10. Histograms of probability mass functions of these symbol sequences are obtained as statistical patterns that indicate evolution of fault growth. Examples are shown in Fig. 4 and Fig. 5 that are histograms of the probability mass functions for test #1 and test #6, respectively.
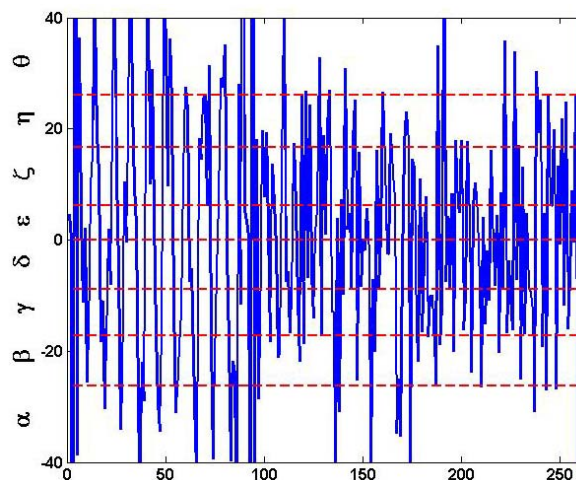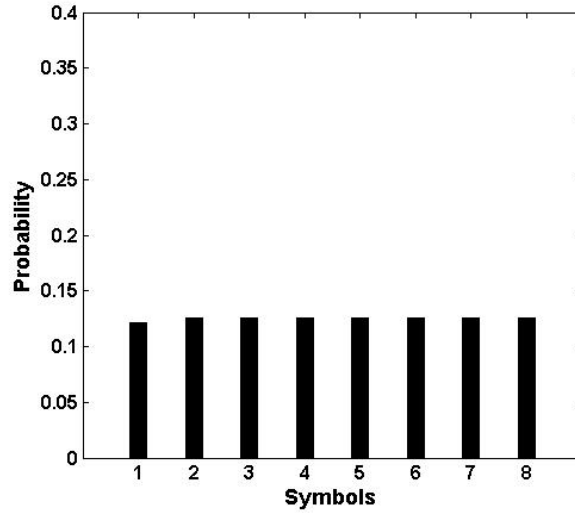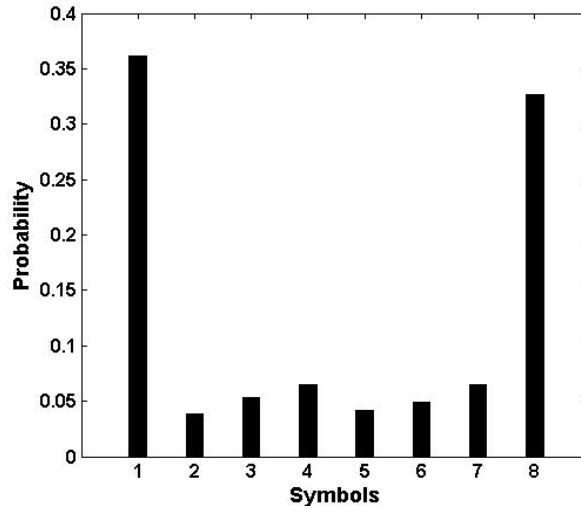

Fig. 3. Maximum Entropy (ME) Partition of DWT Coefficients.

**Fig. 4.** Probability Mass Function (PMF) for Test #1 (Healthy Motor).

Fig. 5. Probability Mass Function (PMF) for Test #6 (Faulty Motor).

It is seen in Fig. 4 and Fig. 5 that the probability distributions of the two tests differ from each other. To quantify the difference, the relative entropy or Kullback-Liebler distance [14] between the distributions has been used as a measure,

$$M_k = -\sum_{i=1}^{i=|\Sigma|} p_i^{\ k} log_2 \frac{p_i^{\ k}}{p_i^{\ 1}}, \qquad (10)$$

where p_i^k is the probability of symbol i in the distribution $\mathbf{p}^k$ distribution corresponding to test #k; and $\mathbf{p}^1$ represents the reference distribution corresponding to test #1, which is uniform as a consequence of maximum entropy partitioning [13]. Consequently, p_i^1's are identically equal to $\frac{1}{|\Sigma|} = \frac{1}{8}$ because $|\Sigma| = 8$ is selected in these tests. It is noted that usage of relative entropy as anomaly measure is not unique; alternative definitions of anomaly measure have been successfully demonstrated in literature [4], [5].

Tests #1 through #5 correspond to five different identical healthy motors while tests #6 through #10 correspond to five similar motors after a single rotor bar was (apparently) identically damaged in each case. The anomaly measures of tests #1 through 5 are very small and the measures are relatively large for tests #6 through #10. The anomaly measures obtained for ten different tests are depicted in Fig. 6, where anomaly measures of the healthy motors are small (< 0.1), which is quite distinct from faulty motors (> 0.48). Therefore, it is inferred that the wavelet-based symbolic approach is capable of distinguishing between healthy and faulty motors. In this case, both probabilities of missed detection and false alarms are very low.
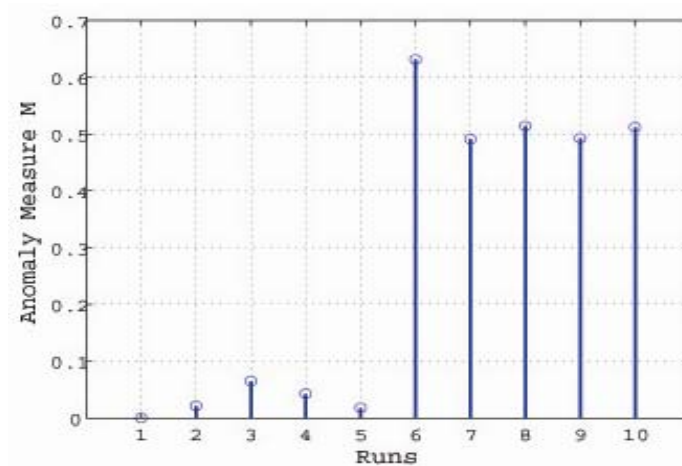
Fig. 6. Anomaly Measure of Experimental Runs.

6. Summary and Conclusions

This paper presents a wavelet-based symbolic dynamic approach [3][13] for detection of both gradually evolving and abrupt faults. This approach makes use of discrete wavelet transform coefficients of the time-domain signal with appropriate choices of the wavelet basis and scales. Then, the sequences of wavelet coefficients are coarse-grained into symbol sequences under partitions generated by the maximum entropy scheme. Histograms of probability mass functions are generated from symbol sequences as statistical patterns of fault evolution. The Kullback-Leibler distance [14] between the statistical patterns (i.e., probability distributions) has been used as a measure of anomalous behavior to detect a fault.

It has been observed that the intelligent sensing method, presented in this paper, is capable of distinguishing the experimental results on a healthy motor from those on a faulty motor with a damaged rotor bar. The computed measures of anomaly are located in distinct frequency bands, which alleviate the issue of false detection.

Results of this investigation suggest that the wavelet based symbolic dynamic approach is a viable analytical tool of intelligent sensing especially for identification of faults or anomalies that have small signatures. However, further theoretical and experimental research is necessary before its industrial application as a part of the Instrumentation & Control system. From this perspective, future research is recommended in the following areas:
- Theoretical research on alternative (e.g., Hilbert transform based [15]) methods for partitioning the data sequences into symbol sequences;
- Application to other types of motor faults such as bearing and stator winding degradation;
- Application to health monitoring and remaining life prediction under varying load conditions.

Acknowledgements

References

[1]. S. Mallat, A Wavelet Tour of Signal Processing, 2nd Edition, *Academic Press*, San Diego, CA, USA, 1998.

[2]. M. Eltabach, A. Charara and I. Zein, A comparison of external and internal methods of signal spectral analysis for broken rotor bars detection in induction motors, *IEEE Transactions on Industrial Electronics*, Vol. 51, No. 1, 2004, pp. 107 – 121.

[3]. A. Ray, Symbolic dynamic analysis of complex systems for anomaly detection, *Signal Processing*, Vol. 84, No. 7, 2004, pp. 1115– 1130.

[4]. S. Chin, A. Ray, and V. Rajagopalan, Symbolic time series analysis for anomaly detection: A comparative evaluation, *Signal Processing*, Vol. 85, No. 9, 2005, pp. 1859 – 1868.

[5]. S. Gupta and A. Ray, Symbolic Dynamic Filtering for Data-Driven Pattern Recognition. Chapter 2 in Pattern Recognition: Theory and Application. IE. A. Zoeller, Nova, *Science Publisher*, Hauppage, NY, USA, 2007.

[6]. S. Gupta and A. Ray, Real-time fatigue life estimation in mechanical systems, *Measurement Science and Technology*, Vol. 18, No. 7, 2007, pp. 1947 – 1957.

[7]. C. Daw, C. Finney, and E. Tracy, A review of symbolic analysis of experimental data, *Review of Scientific Instruments*, Vol. 74, No. 2, 2003, pp. 915 – 930.

[8]. M. E. H. Benbouzid, A review of induction motors signature analysis as a medium for faults detection, *IEEE Transactions on Industrial Electronics*, Vol. 47, No. 5, 2000, pp. 984 – 993.

[9]. D. Diallo, M. Benbouzid, D. Hamad, and X. Pierre, Fault detection and diagnosis in an induction machine drive: A pattern recognition approach based on concordia stator mean current vector, *IEEE Transactions on Energy Conversion*, Vol. 20, No. 3, 2005, pp. 512 – 519.

[10]. A. Teolis, Computational Signal Processing with Wavelets, *Birkhäuser*, Boston, MA, USA, 1998.

[11]. P. Abry, Ondelettes et turbulence. Multirsolutions, algorithmes de dcomposition, invariance d'chelles, *Diderot Editeur*, Paris, France, 1997.

[12]. P. Vaidyanathan, Multirate systems and filter banks, *Prentice Hall*, Englewood Cliffs, NJ, USA, 1993.

[13]. V. Rajagopalan and A. Ray, Symbolic time series analysis via wavelet-based partitioning, *Signal Processing*, Vol. 86, No. 11, 2006, pp. 3309 – 3320.

[14]. T. Cover and J. Thomas, Elements of Information Theory, *Wiley-Interscience*, New York, NY, USA, 1991.

[15]. A. Subbu and A. Ray, Space partitioning via Hilbert transform for symbolic time series analysis, *Applied Physics Letters*, Vol. 92, No. 8, 2008, p. 084107.

_____